J. Neurovirol. (2012) 18:388–399
DOI 10.1007/s13365-012-0120-3

Antiretroviral neurotoxicity

Kevin Robertson · Jeff Liner · Rick B. Meeker

Received: 1 March 2012 / Revised: 26 June 2012 / Accepted: 27 June 2012 / Published online: 19 July 2012

Abstract Combination antiretroviral therapy (CART) has proven to effectively suppress systemic HIV burden, however, poor penetration into the central nervous system (CNS) provides incomplete protection. Although the severity of HIV-associated neurocognitive disorders (HAND) has been reduced, neurological disease is expected to exert an increasing burden as HIV-infected patients live longer. Strategies to enhance penetration of antiretroviral compounds into the CNS could help to control HIV replication in this reservoir but also carries an increased risk of neurotoxicity. Efforts to target antiretroviral compounds to the CNS will have to balance these risks against the potential gain. Unfortunately, little information is available on the actions of antiretroviral compounds in the CNS, particularly at concentrations that provide effective virus suppression. The current studies evaluated the direct effects of 15 antiretroviral compounds on neurons to begin to provide basic neurotoxicity data that will serve as a foundation for the development of dosing and drug selection guidelines. Using sensitive indices of neural damage, we found a wide range of toxicities, with median toxic concentrations ranging from 2 to 10,000 ng/ml. Some toxic concentrations overlapped concentrations currently seen in the CSF but the level of toxicity was generally modest at clinically relevant concentrations. Highest neurotoxicities were associated with abacavir, efavarenz, etravirine, nevaripine, and atazanavir, while the lowest were with darunavir, emtracitabine, tenofovir, and maraviroc. No additive effects were seen with combinations used clinically. These data provide initial evidence useful for the development of treatment strategies that might reduce the risk of antiretroviral neurotoxicity.

K. Robertson · J. Liner · R. B. Meeker (✉)
Department of Neurology, University of North Carolina,
Chapel Hill, NC 27599, USA
e-mail: meekerr@neurology.unc.edu

Keywords HIV · Dementia · Neurons · Therapy · Treatment

Introduction

HIV-1 rapidly enters the central nervous system (CNS) after infection and establishes a persistent viral reservoir. CNS HIV infection frequently results in neurological disease marked by a set of cognitive, motor, and behavioral symptoms known as HIV-associated neurocognitive disorders (HAND) (Antinori et al. 2007). Potent combination antiretroviral (ARV) therapies have been shown to improve cognition and reduce the prevalence of HIV-associated Dementia, the most severe form of HAND (Dilley et al. 2005; Sacktor et al. 2001; Saksena and Smit 2005). Recent studies have shown that mild–moderate neurocognitive manifestations of HIV infection persist in about 40 % of patients on treatment (Sacktor et al. 2002; Villa et al. 1996). In addition, studies indicate that the prevalence of neurocognitive disorders is increasing as patients live longer (Heaton et al. 2011; Robertson et al. 2007). To control viral replication in the brain, strategies are under development to increase the penetration of ARV compounds across the blood–brain barrier (Bressani et al. 2010; Mahajan et al. 2010; Manda et al. 2010; Prabhakar et al. 2011; Saiyed et al. 2010). Although these compounds have well described toxic actions systemically and in the peripheral nervous system (Bartlett and Lane 2012), little is known about the toxicity of the compounds to neurons in the CNS. One recent study reported that cognition improved for up to 96 weeks in a group of immunologically and virologically stable patients who elected to come off of treatment (Robertson et al. 2010). These results raised the possibility that even low concentrations of ARVs that penetrate the brain may have some detrimental effects. If this is true, future efforts at delivering higher concentrations of ARVs

to the CNS will have to take into consideration the potential adverse effects. Careful studies of the effects of ARV compounds at concentrations required to suppress viral replication are needed to evaluate this possibility and to guide the use of compounds that will minimize CNS complications. To provide a comparative analysis of the neurotoxicity of ARV compounds, we evaluated the direct effects of 15 different ARV compounds and six different combinations of ARV compounds on primary cultures of rat neurons.

Methods

Primary cultures of rat forebrain

Fetuses were harvested at E17 from pregnant female Long–Evans rats, washed with ice cold HEPES-buffered Hank's balanced salt solution (HBSS) and the brain removed. The euthanasia and tissue harvest protocols were done in accordance with NIH and institutional guidelines and were approved by the Institutional Animal Care and Use Committee. The cortex/hippocampus was dissected from the brain and cleaned of dura-arachnoid membrane and visible vessels. The tissue was transferred to a 15-ml tube containing 5 ml calcium–magnesium free-HBSS + 2.4 U/ml dispase + 2 U/ml DNase I and incubated for 20–30 min at 37 °C. Tissue was triturated and allowed to settle for 2 min, and the suspended cells were transferred to a 50-ml culture tube containing 25 ml of complete medium (Minimum Essential Medium [MEM] + 10 % fetal bovine serum [Invitrogen, Certified FBS] + 20 μg/ml gentamicin). The trituration/collection cycle was repeated until most of the tissue was dispersed. Dissociated cells were seeded at a density of 20,000–100,000 cells/cm^2 on poly-D-lysine-coated coverslips or 100,000 cells/cm^2 in poly-D-lysine-coated 96-well plates. Cultures were >90 % neurons 3 days after seeding based on morphology and stain for microtubule-associated protein-2 (MAP-2). Cultures were fed by 50 % medium exchange three times a week. Cultures were allowed to mature normally for 6 days without the use of mitotic inhibitors.

Antiretroviral compounds

ARV compounds were obtained through the NIH AIDS Research and Reference Reagent Program, Division of AIDS, NIAID. Concentrated (1,000×–10,000×) stocks were made in water (ddC, ddI, AZT, FTC, TDF, 3TC, ATV, MVC), DMSO (ABC, EFV, NVP, APV, DRV, RTV), or ethanol (ETV) and diluted in culture medium for use (plasma therapeutic concentrations in Table 1 were designated as 1X). Compounds were added to the cultures in concentrations ranging from 0.01 to 300 μg/ml to investigate the dose response of each individual compound. Combinations of compounds were tested using the reported plasma levels for each drug in the combination (see Table 1).

Table 1 Summary of ARV concentrations in plasma and CSF relative to toxic activity in vitro

Drug	Molecular weight	Max % MAP-2 loss	% Threshold TC50	Plasma concentration (ng/ml)	CSF concentration (ng/ml)	Reference
Abacavir (ABC)	286.3	27.2	2.2	139 (median)	128 (median)	Caparelli et al. 2005
2′,3′-Dideoxycytidine (ddC)	211.2	52.5	1065	25.3 (Cmax)	2.1 (Cmax)	ddC package insert
2′,3′-Dideoxyinosine (DDI)	236	42.5	18.4	840 (Cmax)	40 (mean	Burger et al. 1995; Hoetelmans et al. 1998
Emtricitabine [(−) FTC]	247.2	47.3	5287	261 (median)	109 (median)	Best et al. 2009a
Tenofovir (TDF)	305.2	18	80.9	96 (median)	5 (median)	Best et al. 2008
Lamivudine (3TC)	229.3	34.9	193.4	1195 (Cmax)	46 (median)	van Praag 2002
Zidovudine (AZT)	267	42.4	1638	635 (Cmax)	38 (median)	van Praag 2002
Efavirenz (EFV)	315.7	36.5	199.5	2145 (median)	13.9 (median)	Best et al. 2009a
Etravirine (ETR)	435.3	23.1	6.8	875.7 (Cmax)	0.9 (Cmax * 0.001)	Kakuda et al 2008
Nevirapine (NVP)	266.3	34.7	151.2	6199 (Cmax)	932 (median)	van Praag 2002
Amprenavir (APV)	505.6	29.1	49	2150 (median	25 (median)	Letendre et al. 2008
Atazanavir Sulfate (ATV)	802.9	33.5	15.8	1278 (median)	10.3 (median)	Best et al. 2009b
Darunavir (DRV)	593.7	17	10452	3930 (median)	34.2 (median)	Yilmaz et al. 2009
Ritonavir (RTV)	721	31.4	2375	1400 (Cmax)	23	Liu et al. 2007; Kravcik et al. 1999
Maraviroc (MVC)	513.7	22	2978	94.9 (median)	3.6 (median)	Yilmaz et al. 2009

NRTI nucleoside reverse transcriptase inhibitor, *NNRTI* non-nucleoside reverse transcriptase inhibitor, *PI* protease inhibitor, *EI* entry inhibitor, *MAP-2* microtubule associated protein-2, TC_{50} median toxic concentration, *ND* no damage

ARV challenge

At 6 days in culture, the rat cortical neurons were challenged for 1 week with one of 15 ARVs at concentrations ranging from 0.01 to 300 μg/ml to determine single drug toxicities. At 6 days neurons express extensive synaptophysin immunoreactivity and excellent responsiveness to glutamate. The period from 6 to 13 days represents a time in which the neurons are healthy and stable providing a solid baseline for the toxicity studies. Concentrations were chosen to represent a range of at least one order of magnitude above and below the therapeutic plasma concentrations used in patients to suppress HIV replication. A summary of this information is provided in Table 1. In addition, six combinations of ARVs currently in the DHHS guidelines were tested to determine the impact of multiple drugs.

MAP-2 immunostaining for assessment of neuronal loss and damage

Neurons were identified by MAP-2 immunostaining. Cells were fixed in ice cold 97 % methanol, 3 % acetic for 10 min at room temperature and washed in 0.01 M phosphate-buffered saline (PBS, 3×5 min). Cells were incubated in blocking buffer containing 3 % normal goat serum in 0.01 PBS for 60 min at room temp. Polyclonal rabbit anti-MAP-2 (Chemicon/Millipore, Bilerica, MA) was then applied at a dilution of 1:500 in blocking buffer and incubated overnight at 4 °C. The cells were washed three times in PBS and incubated in goat anti-rabbit Alexa488 or mouse anti-rabbit Alexa568 (Molecular Probes/Invitrogen, Carlsbad, CA) at a dilution of 1:500 for 1 h at room temperature. Cells were then washed 3×5 min, counterstained with bis-benzimide (0.5 μM; Sigma, St. Louis, MO) for 20 min in PBS and washed 2×5 min in PBS. Coverslips were mounted onto slides with Fluoromount (Southern Biotech, Birmingham AL) and 96-well plates were filled with 50 % glycerol solution in PBS.

MAP-2 data analysis

Three or four images were digitally captured from each well at a magnification of 193× using the MetaMorph™ System. An intensity threshold was set to highlight the MAP-2 stained neurons and proximal dendrites within each image while limiting background. The thresholded area was then measured as a percent of total area. Neuronal damage typically included beading and pruning of dendrites with a corresponding decrease in MAP-2 staining. The decrease in MAP-2+ processes was apparent in intact neurons and proved to be a very sensitive index of neuronal damage. However, a caveat of this approach is that the use of sensitive measures also introduces greater error in the assessments which must be taken into consideration in the interpretation of the results. The accuracy of estimates from the data was therefore calculated based on the variation seen. Data from each image were averaged for each well within a 96-well plate and then across three to four replicate experiments from different cultures. Concentration–effect curves and an estimate of the median toxic concentration (TC_{50}) were generated from the average data using Graphpad Prism software. Since some damage (e.g., beading of dendrites) may not correlate with decreases in MAP-2 stain intensity, we also confirmed damage by quantifying the extent of beading and by rating the quality of the neurons on a scale of 1 to 10 (10 being very healthy with abundant neurons and intact processes, 5 representing abundant, well stained neurons with moderate beading and/or loss of dendrites and 1 representing an almost complete loss of MAP-2+ neurons). The bead density correlated well with the MAP-2 stain intensity values (r=0.534±0.036) indicating that the beading paralleled changes in the density of the processes. Thus, the independent influence of beading in the analysis was small. In addition, the qualitative ratings verified that the MAP-2 quantification matched the visible damage to the neurons. Over the concentrations studied, no treatments resulted in complete loss of MAP-2 staining. Thus, the TC_{50} value reflects the relative potency of the compound but not the total amount of damage. The maximum amount of MAP-2 loss or damage was recorded separately to provide an estimate of the extent of damage.

Correction for DMSO damage

Several of the drugs used were not soluble in aqueous solutions and were therefore dissolved in DMSO to make the stock solutions. These stocks were prepared at concentrations 1,000 to 10,000 times the therapeutic concentration to minimize toxicity of the vehicle. However, to provide an accurate correction for toxicity of the DMSO, a dose response curve was run on each plate. The dose–response curve for both the Metamorph MAP-2 stain measurements (% threshold) and visual damage assessments are illustrated in Fig. 1. Values represent mean ± SEM. In addition, the DMSO dose–response curve for loss of mitochondrial activity based on conversion of MTT is shown. In each case, there was no consistent DMSO toxicity until concentrations exceeded 0.44 % (log % = −0.356, the point at which the best-fit curve begins to drop). By 4 % there was extensive loss of MAP-2 stain (52–88 %), neuron integrity and MTT conversion. Toxicity due to DMSO was subtracted from each compound at the matched concentration to provide the best estimate of the toxicity of the compound. Concentrations with DMSO greater than 1 % (0 value for log DMSO) were not included in the TC_{50} calculations.

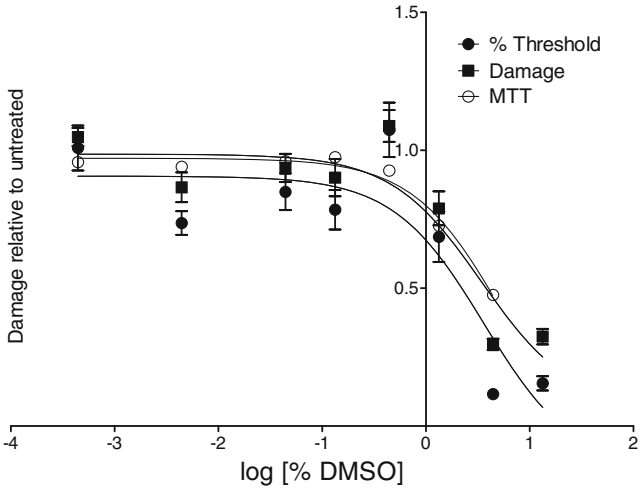

Fig. 1 DMSO toxicity dose–response curve. Neuronal toxicity due to DMSO relative to untreated controls was similar in three different analyses which measured the area occupied by MAP-2 stained cells (% threshold), damage scores based on morphology of MAP-2 stained cells (damage) and results from an MTT assay for mitochondrial activity. In each case, damage was first apparent after reaching a concentration of 1 % DMSO (log DMSO=0). Values are mean ± SEM

Calculation of the toxicity index and toxicity risk

To provide a relevant endpoint, we asked whether the toxic effects seen in vitro occurred at ARV concentrations achieved in patients on ARV therapy. The toxicity index was calculated as the log of the reported therapeutic plasma concentration divided by the estimated TC_{10} value from the data in Fig. 3. A concentration one log lower than the TC_{50} was used to provide an estimate of the toxicity threshold and corresponded to about 10 % loss of the MAP-2 stain (TC_{10}). A value of 0 was obtained when the TC_{10} was equal to the therapeutic plasma concentration in Table 1. Negative values reflect favorable toxicity profiles while positive values reflect less favorable profiles. Toxicity risk was estimated in the same fashion from current estimates of ARV concentrations in the CSF. Values greater than or equal to 0 indicate that concentrations in the CSF under current treatment conditions are in the toxic range.

Antiretroviral compounds and glutamate-induced changes in intracellular calcium

Neuronal cultures were incubated for 2 days in medium containing ARV compounds at concentrations that matched the therapeutic concentrations in plasma. Cells were then transferred to HEPES-buffered artificial CSF (aCSF: NaCl 137 mM, KCl 5.0 mM, $CaCl_2$ 2.3 mM, $MgCl_2$ 1.3 mM, glucose 20 mM, HEPES 10 mM, adjusted pH 7.4 with NaOH) and pre-loaded with the calcium indicator dye Fluo-4 NW (1:4 dilution; Molecular Probes/Invitrogen) in serum-free medium at 37 °C. After 30 min, the coverslip was transferred to a specialized stage for imaging (Warner Instruments). Time lapse digital images were captured automatically by the Metamorph system. Three pre-stimulation images were taken to establish baseline calcium in each cell. In some experiments, the acute and delayed response to glutamate was then measured after the application of 10 μM glutamate to the chamber. The increase in fluorescence intensity was then calculated relative to the baseline fluorescence for each neuron within the field to correct for any differences in dye loading or intrinsic fluorescence. Data from several runs was consolidated and the average cellular response and standard error calculated.

Estimates of mitochondrial membrane potential with TMRM and MTT

To image changes in mitochondrial membrane potential at high resolution, neuronal cultures on coverslips at 20,000 cells/cm^2 were incubated for 2 days with ARV compounds and then 100 nM tetramethylrhodamine methyl ester (TMRM) was added to the medium. Cultures were incubated for 10 min at 37 °C and the neuronal mitochondria imaged at 1680× in aCSF using the MetaMorph™ System. The intensity of stain was measured, averaged across cells and compared between compounds. Images of the stained mitochondria were taken to provide an indication of changes in morphology. Higher throughput analyses for dose–response studies were conducted using MTT conversion in 96 well plates at a neuron density of 10^5 cells/cm^2. Briefly, 10 μl of a 12 mM stock of MTT in PBS was added to 100 μl of culture medium and the cells were incubated at 37 °C for 2 h. The medium was then removed and 50 μl of DMSO added to each well. After mixing, the plate was incubated at 37 °C for 10 min. The plate was again mixed and the OD of the solution measured on a plate reader at 540 nm.

Results

Antiretroviral compounds have a wide range of neurotoxic potencies

Examples of the types of damage seen in neural cultures treated for 7 days with ARV compounds are illustrated in Fig. 2. Untreated cultures have large, well stained MAP-2+ neurons (green) with elaborate outgrowth of processes (Fig. 2a). In general, the ARVs were not highly toxic. Typical damage included beading (Fig. 2b), simplification of the dendritic processes (Fig. 2c), and neuronal shrinkage. The images illustrate changes in response to efavirenz

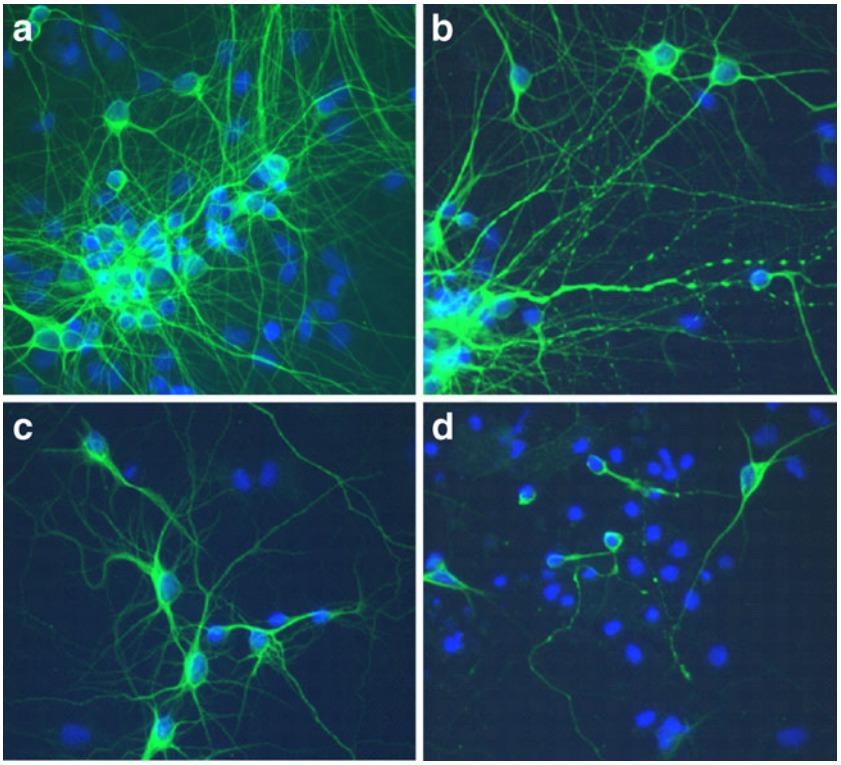

Fig. 2 Examples of the types of damage seen and measured in neural cultures treated for 1 week with efavirenz or atazanavir. Neurons were stained for MAP-2 (*green*) and counterstained with the nuclear stain, bisbenzimide (*blue*). The images illustrate the types of damage that contribute to toxicity but were not matched for neuron density and do not necessarily reflect the average extent of damage for the compounds illustrated since cultures often contained a mix of each type of damage. **a** Untreated cultures contained healthy neurons with extensive outgrowth of processes. **b** Beading of the dendrites was an early sign of damage and often appeared adjacent to other normal looking neurons (7 days efavirenz). **c** Some neurons showed normal cell bodies but had less extensive elaboration of dendrites relative to matched untreated cultures (7 days atazanavir). **d** The most severe damage such as shrinkage of the neuropil and an extensive loss of dendrites was seen only at the highest concentrations of some drugs (efavarenz at 30 μg/ml) and was generally confounded by the presence of high concentrations of DMSO. However, similar elements could be seen in many cultures with less severe overall damage. In each case, the damage causes a loss of area occupied by MAP-2 stained neurons which could be quantified to provide a measure of toxic damage in live neurons

(Fig. 2b, d) or atazanavir (Fig. 2c) but are representative of all ARVs. Extensive cell death and damage was only seen at the highest concentrations of some compounds (Fig. 2d; efavarenz, 300 μg/ml) and was confounded by the toxicity of DMSO. Most cultures showed a combination of effects (e.g., beading and pruning) which resulted in a loss of MAP-2 stained processes which could be measured by a decrease in the area occupied by MAP-2+ cells and processes. The ability of the measures of MAP-2 staining to track with damage to the neurons was verified using blinded ratings of the quality of the neural cultures on a scale of 1–10 (1 = extensive damage and loss of MAP-2 stain, 10 = no damage, excellent stain). The damage ratings closely paralleled the MAP-2 analysis but were generally less sensitive than the quantitative measures of MAP-2 density.

The curves in Fig. 3 illustrate the change in total area of MAP-2+ cells and processes relative to the vehicle-treated control cultures with increasing concentrations of each compound. To provide a comparison to concentrations present in vivo, we have included a solid vertical line to indicate the concentration reported in plasma of patients on therapy. Concentrations measured in CSF are indicated by the dashed vertical line. The median toxic concentration (TC_{50}) calculated from these curves for each compound is summarized in Table 1. The maximum loss of MAP-2 immunoreactivity is also included to indicate the extent of damage since each compound induced only a partial loss of neuron staining over the concentrations tested. The NRTI's ddC, DDI, FTC and AZT induced the greatest amount of damage (42–52 % loss of MAP-2). The NNRTI's and the protease inhibitors generally produced less total loss of MAP-2 (17–36 %). DRV, MVC and TDF produced the least amount of damage (17–22 %). Cell death was assessed by a semi-automated count of small condensed bisbenzimide stained nuclei using Metamorph integrated morphometry. The relative number of nuclei consistent with dead or apoptotic cells ranged from 0.4 % to 2.5 % for the 15 compounds compared to 1.6±0.9 % for vehicle controls. The highest values (ABC 1.4 %, 3TC 1.7 %, EFV 1.9 % and ATV 2.5 %) were generally consistent with the MAP-2 results but

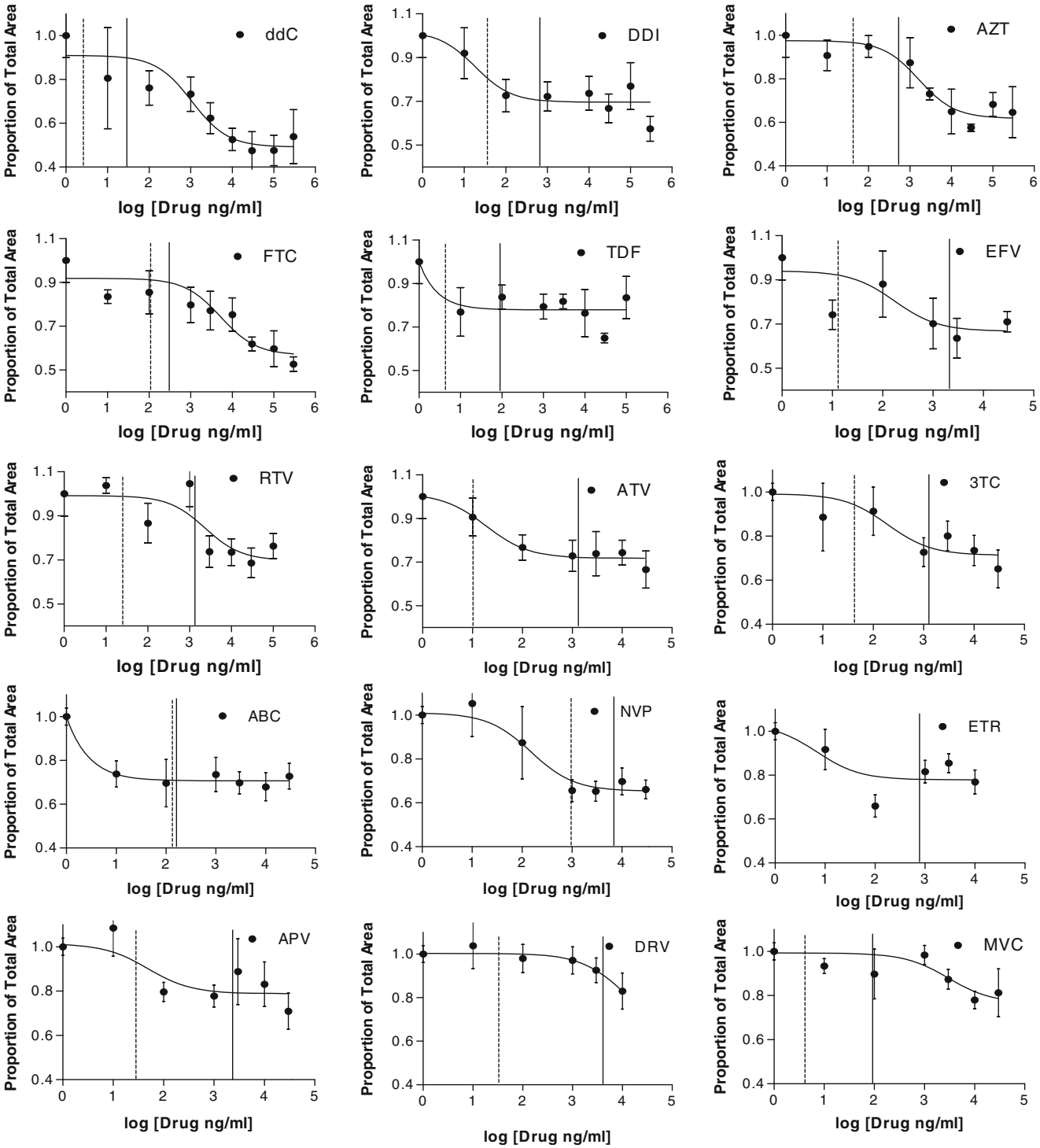

Fig. 3 Dose–response curves for damage induced by each of 15 different antiretroviral compounds incubated in neural cultures for 1 week (day 6 to day 13). The proportion of total area occupied by MAP-2 stained neurons and processes relative to untreated control cultures is plotted versus the log of the drug concentration (ng/ml). The best-fit sigmoidal curve was determined using Graphpad Prism software and was used to calculate the median toxic concentration (TC_{50}) for each compound which is summarized in Table 1. The shape and midpoint of the curves varied widely between compounds indicating variable toxic properties. No compound caused a complete loss of MAP-2 immunoreactivity at the concentrations tested with the loss ranging from 17 % to 52 %. *Solid lines* indicate the therapeutic concentration reported in plasma of HIV patients. *Dashed lines* indicate the reported concentration in the CSF. Values are mean ± SEM

no changes were significantly different from controls and all were in the range of normal cell death typically seen in these cultures. Therefore, cell death contributes very little if at all to the neurotoxicity.

Therapeutic concentrations of most ARVs would be predicted to have moderate neurotoxic activity

To generate a profile of relative toxicities, a toxicity index was calculated for each compound. To provide a conservative estimate of potential toxicity, we elected to base the toxicity index on the lowest concentration at which toxicity might begin to develop. A threshold concentration one log lower than the TC_{50} was chosen to represent approximately a 10 % drop in the MAP-2 intensity (TC_{10}). The log transform of the plasma concentration seen in patients on therapy divided by the TC_{10} is illustrated in Fig. 4a. A score of 0 on this scale is obtained when the therapeutic plasma concentration is equal to the TC_{10} (the toxic threshold). Negative scores reflect less neurotoxicity and positive scores greater neurotoxicity. Based on this analysis, eight compounds (ABC, DDI, 3TC, EFV, ETR, NVP, APV and ATV) have a relatively high risk of neurotoxic effects (index = 1.79–3.11) assuming plasma levels were achieved in CNS. TDF, AZT, DRV and RTV have a lower risk of toxicity (index = 0.58–1.07) and ddC, FTC and MVC would be predicted to have no significant toxic effects (index ≤0). To provide an estimate of the potential risk of toxicity given current values for CSF penetration of each compound, the TC_{10} was divided by the reported CSF concentration for each drug. In this case, values greater than or equal to 0 indicate that CSF concentrations are potentially high enough to produce neuronal damage. Based on this assessment, three compounds (ABC, DDI, NVP) have a relatively high potential risk (index = 1.34–2.76). 3TC, ETR, APV and ATV have some low risk (index = 0.12–0.81), whereas ddC, FTC, TDF, EFV, DRV, RTV and MVC have no predicted risk (index <0).

Combinations of antiretroviral drugs did not have additive neurotoxic effects

To determine if combination ARV therapy poses an increased risk of neurotoxicity, we challenged neurons with six different combinations. The plasma concentration from Table 1 was used for each compound. The loss of MAP-2 immunoreactivity after 7 days is summarized in Fig. 5 relative to matched, untreated cultures. The amount of damage at therapeutic concentrations was not extensive suggesting that the combinations did not have additive neurotoxic effects. The greatest loss of MAP-2 immunoreactivity was seen for the combination, ATV, RTV, TDF, FTC (28.8 %), followed by DRV, ABC, 3TC (24.6 %), EFV, ABC, 3TC (17.1 %) and NVP, TDF, FTC (12.5 %). The combinations EFV, TDF, FTC and DRV, TDF, FTC did not produce significant damage. The density of neurons/mm^2 did not change (range = 216±8 to 241±12/mm^2) indicating that there was no significant neuronal loss under these conditions. The low level of cell death was verified by an analysis of condensed and fragmented bisbenzimide stained nuclei indicative of apoptotic cells. The relative number of nuclei with apoptotic profiles ranged from 1.55±0.79 % to 3.01±0.35 % versus 1.15±0.60 % for untreated cultures. Although no changes were significantly different from controls, an inverse correlation was seen between MAP-2 density and apoptotic nuclei (r=−0.766), suggesting a possible small effect on cell viability.

Different ARV combinations may either sensitize or desensitize neurons to the toxic actions of glutamate

To evaluate the functional response of neurons after exposure to ARV combinations for 2 days, we challenged

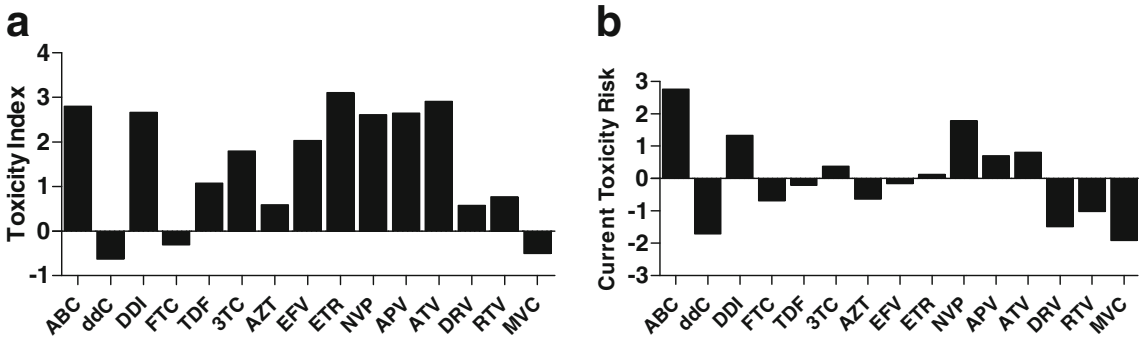

Fig. 4 Illustration of the estimated toxicity index and toxicity risk for each of 15 antiretroviral compounds. To reflect the threshold concentration at which toxicity might first begin to develop, the toxicity index was calculated as the log of the reported therapeutic plasma concentration divided by the estimated TC_{10} value from the data in Fig. 3. **a** Six compounds had a toxicity index >2 and three more an index >1 indicating a relatively high risk of toxic effects from most compounds. AZT, DRV and RTV had a modest index between 0 and 1 while ddC, FTC and MVC had negative values indicating a relatively low risk of neural damage at therapeutic concentrations. **b** Toxicity risk was estimated in the same fashion from the current estimates of ARV concentrations in the CSF. ABC, DDI, and NVP had values >1 (1.34–2.76), indicating significant current risk of toxicity. APV (0.71) and ATV (0.81) had a low risk of toxicity, whereas all other compounds had negligible risk of toxicity based on this assessment

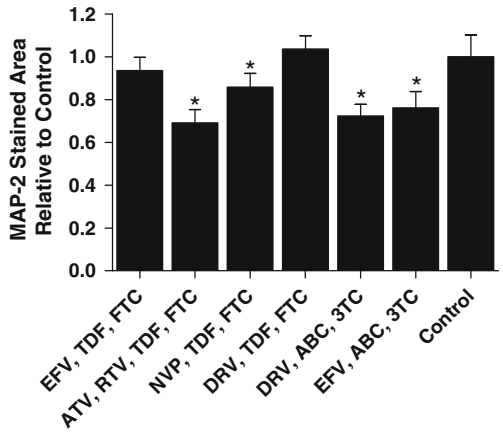

Fig. 5 Loss of MAP-2 stain in neural cultures treated for 7 days with one of five different antiretroviral combinations relative to untreated cultures. The concentration of each drug was matched to the therapeutic plasma concentration in Table 1. Four combinations significantly decreased the MAP-2 stained area (*$p<0.05$), although the extent of damage was moderate with a maximum loss of 31 % of the MAP-2 stained area. Values are mean ± SEM

the neurons with a moderate concentation of glutamate (10 μM) and measured both the acute and delayed intracellular calcium response (Fig. 6). The mean peak calcium response to glutamate was 508±51 brightness units above baseline. Drug combinations that produced the greatest damage (DRV, ABC, 3TC) showed larger acute and delayed increases in intracellular calcium in response to glutamate. Combinations with more moderate toxicity (ATV, RTV, TDF, FTC) showed unaltered acute responses to glutamate but a significant delayed response. A less toxic combination (EFV, TDF, FTC) showed a decreased acute response to glutamate followed by a small delayed increase. When neural cultures were challenged acutely with the most toxic combination, DRV, ABC, 3TC, in the absence of glutamate no change in intracellular calcium was seen relative to the aCSF controls. Thus, although the ARVs alter neuronal responsiveness to excitatory neurotransmission, they have no direct effect on calcium accumulation.

Toxicity did not correlate with changes in the mitochondrial membrane potential

Since damage to mitochondria is a known effect of NRTIs (Kline et al. 2009; Lewis et al. 2006; Moyle 2005; Saitoh et al. 2007, 2008; Venhoff et al. 2007), we assessed changes in the mitochondrial membrane potential in response to selected ARVs using the dye TMRM and MTT assays of mitochondrial viability. Two NRTIs (DDI, TDF) with high toxic potential, one NNRTI (EFV) with moderate toxic activity, one PI with high toxicity (ATV) and one PI with low toxicity (RTV) were selected for a high resolution analysis of mitochondria after acute exposure for 2 days. Examples of the staining with the membrane potential probe, TMRM, are shown in Fig. 7a. TMRM intensity was variable, as illustrated by the mean values in Fig. 7b and the distribution of intensities in Fig. 7c, but no clear relationship was seen to neurotoxic activity. The

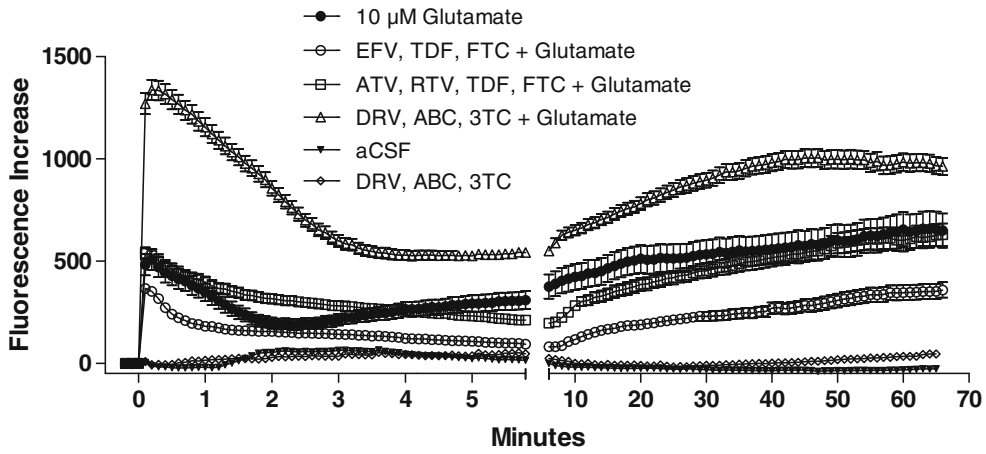

Fig. 6 Neuronal calcium responses to a 10 μM glutamate challenge after incubation in the indicated antiretroviral cocktail for 2 days. The mean fluorescence of neurons loaded with the calcium indicator dye Fluo-4 was measured over time. Fluo-4 fluorescence is proportional to the intracellular calcium concentration. A robust acute response to glutamate was seen in the control neurons (*filled circles*) receiving no antiretroviral treatment followed by a slight rise in the delayed phase. Pre-treatment of the neurons with the ARV combination ATV, RTV, TDF, FTC (*open squares*) resulted in a similar acute and delayed response. Pre-treatment with the more toxic combination of DRV, ABC, 3TC (*open triangles*) resulted in a much greater acute response followed by a larger delayed accumulation of calcium. The less toxic combination of EFV, TDF, FTC (*open circles*) reduced the magnitude of the acute response to glutamate. Although the net accumulation of calcium was lower, the rate of accumulation in the delayed phase was similar to the other ARV combinations. Neurons directly challenged with the ARV cocktail (DRV, ABC, 3TC; *open diamonds*) in the absence of glutamate had no effect on intracellular calcium and were indistinguishable from aCSF controls

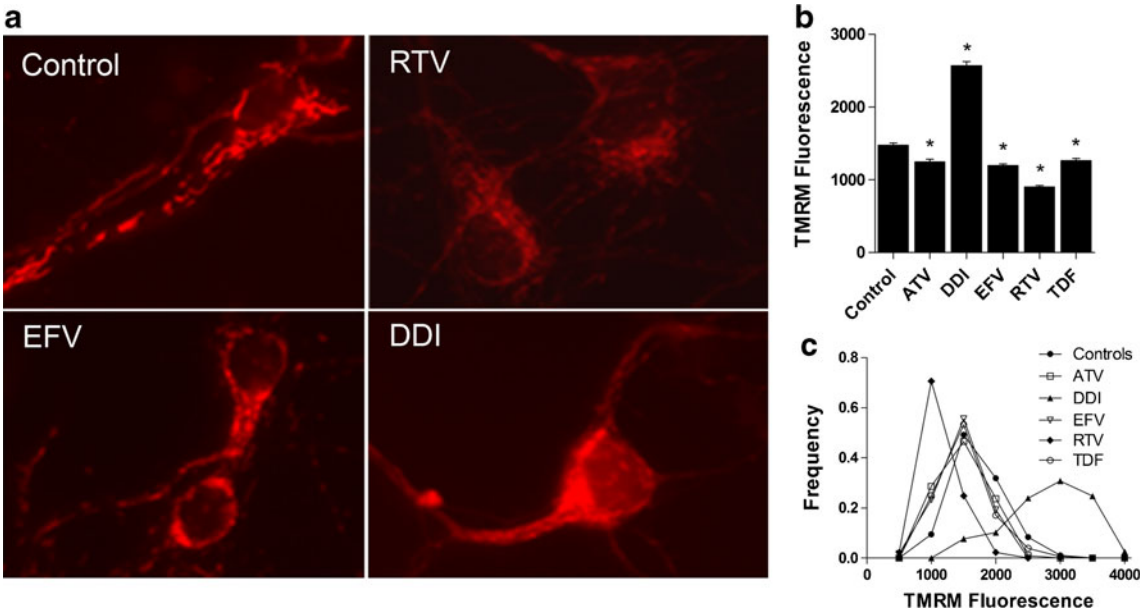

Fig. 7 **a** Examples of cultured neurons stained with the mitochondrial potential sensitive dye TMRM. Control mitochondria were seen as brightly stained, long fingerlike structures in the neurons. Treatment with RTV depleted the mitochondrial membrane potential as indicated by the low intensity of the TMRM stain. EFV had a small effect on the intensity of TMRM. DDI induced an increase in the TMRM fluorescence indicating an increase in the mitochondrial membrane potential. Each compound tested caused a slight rounding of the mitochondria. **b** Quantification of the average TMRM fluorescence in neurons treated with different ARVs. All ARVs tested resulted in a significant decrease in the TMRM fluorescence with the exception of DDI which increased the fluorescence (*$p<0.05$). **c** A frequency analysis illustrating the shift in the distribution of TMRM intensities for each ARV. Most ARVs induced a small shift to the left (decrease in mitochondrial membrane potential). RTV induced the largest shift to the left, whereas DDI produced a notable shift to the right

least toxic compound tested (RTV) had the lowest TMRM staining whereas NRTIs with relatively high toxicity displayed either increased (+74.2 %, DDI) or decreased (−15.6 %, ATV) staining. Changes in mitochondrial morphology were seen under all treatment conditions. The morphology changed from the typical long fingerlike structures to slightly more rounded structures, particularly within the cell body. Again there was no clear relationship between mitochondrial morphology and TMRM intensity or neurotoxicity.

To further evaluate if mitochondrial changes might emerge with longer treatments, five NRTIs (ddC, ddI, FTC, TDF, AZT) expected to have effects on mitochondria, one NNRTI (EFV) and two protease inhibitors (ATV, RTV) were added to neural cultures at eight different concentrations and incubated for a period of 1 week. The cells were then tested using the MTT assay as a quantifiable index of mitochondrial activity and the dose–response relationship evaluated. None of the conditions showed changes in MTT conversion in response to ARV treatment at doses up to 10 μg/ml (not shown). MTT tetrazolium product OD values ranged from 0.185 to 0.203 versus 0.178 to 0.204 for vehicle-treated cultures and the dose–response curve was flat (not shown) with the exception of decreases at high concentrations which could be attributed to the effects of DMSO (e.g., see Fig. 1).

Discussion

Eradication of HIV from the CNS reservoir has been difficult due, in part, to the poor penetration of ARV compounds across the blood–brain barrier. HIV within the CNS continues to produce damage and is a source of infectious virus (Schnell et al. 2009, 2010; Smit et al. 2004). Protection of the brain and elimination of the CNS viral reservoir are high priorities in the treatment of HIV. As newer compounds and methods are developed that improve delivery across the blood–brain barrier, more consideration will have to be given to potential neurotoxicity. Numerous studies indicate that long-term HAART treatment is associated with a range of adverse effects including hepatic steatosis, neuropathy, cardiomyopathy, pancreatitis, lactic acidosis, ototoxicity, retinal lesions and possibly lipodystrophy (Bartlett and Lane 2012). Many of these effects are thought to be associated with the loss of mitochondrial DNA resulting from NRTI inhibition of mitochondrial DNA polymerase gamma (Kakuda 2000). However the mechanisms that give rise to the damage are not well understood and in some cases damage to cells does not correlate with mitochondrial DNA depletion (Kline et al. 2009; Maagaard et al. 2006; Maagaard and Kvale 2009). Substantial differences in NRTI toxicity have been noted between different tissues reinforcing the need to examine the direct effects on neural tissue.

Our in vitro studies provide a comparison of the relative neurotoxicity of different ARV compounds using measures of neuronal dysfunction that are sensitive and designed to reflect the earliest forms of HIV-associated damage. The studies were optimized to measure direct effects of the compounds on neurons. However, it is important to note that this is but one of many possible endpoints that may be relevant. These studies cannot address the potential impact of long-term exposure (months to years) or potential interactions in vivo that may affect neurotoxicity. Nevertheless, these studies begin to provide information on potential risks associated with CNS penetration of ARVs.

Neurotoxicity of individual ARVs ranged from undetectable to moderate and was not due to neuron death

No compound was highly toxic but neural damage in the form of dendritic beading and pruning was a common observation. This pathology was reflected in the loss of MAP-2 staining. Since beading and pruning have been documented under a variety of pathological conditions (Bellizzi et al. 2005; Greenwood et al. 2007; Takeuchi et al. 2005), they most likely reflect a general endpoint associated with neuronal dysfunction (Greenwood et al. 2007; Kim et al. 2010; Masliah et al. 1992). Under these in vitro test conditions, a wide range of median toxic concentrations (TC_{50}) was seen with a low value of 2.2 ng/ml and high values of >5 μg/ml (Table 1). The TC_{50} of ABC, ddI, and NVP fell within the range of concentrations seen in CSF of patients on ARV therapy. The median toxic concentration of ABC, APV, ATV, ddI, EFV, ETR, NVP, RTV, TDF and 3TC, fell within the range of concentrations seen in the plasma suggesting that they may have significant neurotoxic effects if present in CNS at therapeutic concentrations. DRV, FTC, and MVC produced little toxicity at relevant plasma and CSF concentrations. The ratio of the therapeutic plasma concentration to the TC_{10} provided an index of the potential toxicity at concentrations that would suppress HIV replication. The TC_{10} value was used to reflect the earliest drop in the dose–response curve (approximately a 10 % decrease) in an effort to provide a conservative estimate of the concentration at which toxicity might begin. Twelve of the compounds were above this theoretical threshold and some exceeded the threshold by two logs. The range was greater than three logs indicating considerable variation in the relative risk. The lower toxicity indices for ddC, FTC, DRV, RTV and MVC indicate that it may be possible to deliver therapeutic concentrations of some drugs into the CNS with minimal relative risk.

The ratio of the CSF concentration of each drug to the TC_{10} provided an index of the risk of toxicity based on current use. The relatively high penetration of ABC and NVP yielded toxicity risk values much greater than zero indicating that they may be present in CSF at levels capable of producing neurotoxicity. DDI, 3TC, APV and ATV also had scores greater than zero but the predicted amount of toxicity would be minimal. Even in cases where higher levels of toxicity were seen, it is noteworthy that the toxic effects were not due to cell death. The toxic effects associated with dendrite beading and possibly pruning are likely to be reversible, raising the possibility that neuroprotective treatments may be effective in preventing or reversing ARV-associated damage.

Acute effects of the ARVs on neurons may be unrelated to effects on mitochondria

Of the few studies that have looked at the effects of ART on neural tissue. A recent study by Divi et al. (2010) in year-old patas monkey offspring treated in utero with various NRTIs showed a 28.8–51.8 % depletion of mitochondrial DNA. Similar depletion was seen in the liver, suggesting a similar susceptibility between brain and liver. Most toxicity studies have focused on the ability of NRTIs to cause a long-term suppression of mitochondrial DNA through the inhibition of mitochondrial DNA polymerase gamma. However, these compounds also have effects on the ADP/ATP translocator and adenylate kinase, suggesting that other effects may contribute to toxicity (Ciccosanti et al. 2010; Kakuda 2000). Primary neural cultures limit the ability to do long-term studies but clearly demonstrate that damage can be seen with exposures of 2–7 days. Some studies in cell lines have shown that long-term exposure to NRTIs was necessary to deplete mitochondrial DNA and damage cells (Kline et al. 2009), whereas other studies have shown significant depletion of mitochondrial DNA in myoblasts and myotubes by ddI (Saitoh et al. 2008) and human hepatoma cells by various NRTIs (Venhoff et al. 2007) with more modest exposures of 5–25 days. Large tissue differences in the sensitivity to NRTIs have been reported. Based on the slow turnover of mitochondrial DNA in neurons one might expect that they would be less sensitive to the effects of the NRTIs (Wang et al. 1997). The relatively rapid appearance of damage within 7 days in our primary neural cultures and minimal changes in markers of mitochondrial function suggests that other factors may contribute to toxicity. This possibility is consistent with in vitro studies of synaptosomes and isolated mitochondria incubated with CSF achievable concentrations of ddC (6–11 ng/ml) (Opii et al. 2007). Signs of oxidative stress, release of cytochrome *C* and a reduction in anti-apoptotic proteins were apparent within 6 h. Thus, further analyses of ARV toxicity should explore various potential mechanisms of action of the ARV compounds.

Damage was not restricted to the NRTIs as the NNRTIs and PIs also produced damage equal to or greater than the NRTIs. Less is known about the potential neurotoxicity of NNRTIs and PIs although both are associated with

significant side effects. All NNRTIs tested in our studies had neurotoxic potencies that were comparable to the NRTIs. This translated to a high toxicity index for all NNRTIs. The PIs had a wider range of potencies with DRV showing very low neurotoxic potency relative to APV and ATV. This was associated with a favorable toxicity index for DRV. RTV was also less toxic than APV and ATV but slightly more toxic than DRV. The fusion inhibitor, maraviroc (MVC) had a relatively low neurotoxic potency and the lowest toxicity index of all drugs tested. Distinctive differences in the potential neurotoxicity of various PIs and entry inhibitors indicate that a rational selection of ARVs may minimize CNS side effects.

Antiretroviral combinations did not have additive toxic effects

ARV combinations at estimated plasma concentrations produced similar types of damage as seen with individual compounds with little indication of strong additive effects. In some combinations, compounds with a favorable toxicity index appeared to offset the deleterious effects of compounds with a high toxicity index. This was seen not only in the neuronal damage but also in the calcium signaling of neurons in response to glutamate. This observation is similar to studies by Venhoff et al. (2007), where TDF and 3TC attenuated ddI cytotoxicity in human hepatoma cells. These observations indicate that neurotoxicity may be controlled not only by selecting compounds based on their individual properties but also based on interactions between compounds. The ability of the combination of EFV, TDF, FTC to suppress calcium signaling in response to a glutamate challenge raises the possibility that particular combinations could offer some level of protection by reducing the delayed accumulation of calcium. However, the potential impact of the acute "protective" effects will not be entirely clear until we have a better understanding of the toxic mechanisms.

Comparison of ART toxicity to HIV-associated neuronal damage

While the intent of these studies was to identify potential toxic interactions of ARVs with neurons using sensitive measures of neuronal dysfunction, it is important to weigh the potential benefit against the risks. When compared to conditions that recapitulate the toxic effects of HIV under the same culture conditions, the effects of the ARVs are small. For example, direct effects of the ARVs on calcium homeostasis are small relative to the large changes following exposure of the neurons to conditioned medium from HIV-treated human monocyte-derived macrophages.

Estimates of the loss of MAP-2 immunoreactivity at plasma concentrations ranged from approximately 9 % to 28 %. This contrasts with losses of approximately 70 % under conditions that mimic HIV infection in vitro (unpublished data). Based on these in vitro studies, the risk of ARV-associated damage in the CNS relative to the risks of HIV infection would appear to be low.

Conclusions

As we develop new antiviral approaches to target HIV in the CNS greater attention to strategies that minimize the risk to neurons will be needed. Our studies indicate that there is a risk of direct neurotoxic interactions that varies substantially between compounds and that informed selection of ARVs and ARV combinations used to target the CNS may minimize adverse effects. While these data begin to identify potential risks, they should not be viewed as guidelines for the clinical use of ARVs. Similar studies will need to correlate in vitro measures to clinical observations to establish the validity of the in vitro toxicity measures. In addition, long-term effects of the compounds may give rise to other forms of damage and will need to be evaluated. Our ability to make rational choices for therapies directed to the CNS is currently limited by a paucity of data on the complex interactions of ARV compounds with neural tissue. Our studies presented here illustrate that the potential for neural damage and dysfunction is significant and highlight the need for further exploration of the mechanism of neurotoxicity of these compounds individually and in combinations.

Acknowledgements Antiretroviral compounds were obtained through the AIDS Research and Reference Reagent Program

References

Antinori A, Arendt G, Becker JT, Brew BJ, Byrd DA, Cherner M, Clifford DB, Cinque P, Epstein LG, Goodkin K, Gisslen M, Grant I, Heaton RK, Joseph J, Marder K, Marra CM, McArthur JC, Nunn M, Price RW, Pulliam L, Robertson KR, Sacktor N, Valcour V, Wojna VE (2007) Updated research nosology for HIV-associated neurocognitive disorders. Neurology 69:1789–1799

Bartlett JC, Lane HC (2012) Panel on Antiretroviral Guidelines for Adults and Adolescents. Guidelines for the use of antiretroviral agents in HIV-1-infected adults and adolescents. Department of Health and Human Services, Office of AIDS Research, pp 1–166. http://www.aidsinfo.nih.gov/contentfiles/lvguidelines/adultandadolescentgl.pdf

Bellizzi MJ, Lu SM, Masliah E, Gelbard HA (2005) Synaptic activity becomes excitotoxic in neurons exposed to elevated levels of platelet-activating factor. J Clin Invest 115:3185–3192

Bressani RF, Nowacek AS, Singh S, Balkundi S, Rabinow B, McMillan J, Gendelman HE, Kanmogne GD (2011) Pharmacotoxicology of monocyte–macrophage nanoformulated antiretroviral drug uptake and carriage. Nanotoxicol 5:592–605.

Ciccosanti F, Corazzari M, Soldani F, Matarrese P, Pagliarini V, Iadevaia V, Tinari A, Zaccarelli M, Perfettini JL, Malorni W,

Kroemer G, Antinori A, Fimia GM, Piacentini M (2010) Proteomic analysis identifies prohibitin down-regulation as a crucial event in the mitochondrial damage observed in HIV-infected patients. Antivir Ther 15:377–390

Dilley JW, Schwarcz S, Loeb L, Hsu L, Nelson K, Scheer S (2005) The decline of incident cases of HIV-associated neurological disorders in San Francisco, 1991–2003. AIDS 19:634–635

Divi RL, Einem TL, Fletcher SL, Shockley ME, Kuo MM, St Claire MC, Cook A, Nagashima K, Harbaugh SW, Harbaugh JW, Poirier MC (2010) Progressive mitochondrial compromise in brains and livers of primates exposed in utero to nucleoside reverse transcriptase inhibitors (NRTIs). Toxicol Sci 118:191–201

Greenwood SM, Mizielinska SM, Frenguelli BG, Harvey J, Connolly CN (2007) Mitochondrial dysfunction and dendritic beading during neuronal toxicity. J Biol Chem 282:26235–26244

Heaton RK, Franklin DR, Ellis RJ, McCutchan JA, Letendre SL, Leblanc S, Corkran SH, Duarte NA, Clifford DB, Woods SP, Collier AC, Marra CM, Morgello S, Mindt MR, Taylor MJ, Marcotte TD, Atkinson JH, Wolfson T, Gelman BB, McArthur JC, Simpson DM, Abramson I, Gamst A, Fennema-Notestine C, Jernigan TL, Wong J, Grant I (2011) HIV-associated neurocognitive disorders before and during the era of combination antiretroviral therapy: differences in rates, nature, and predictors. J Neurovirol 17:3–16

Kakuda TN (2000) Pharmacology of nucleoside and nucleotide reverse transcriptase inhibitor-induced mitochondrial toxicity. Clin Ther 22:685–708

Kim JY, Shen S, Dietz K, He Y, Howell O, Reynolds R, Casaccia P (2010) HDAC1 nuclear export induced by pathological conditions is essential for the onset of axonal damage. Nat Neurosci 13:180–189

Kline ER, Bassit L, Hernandez-Santiago BI, Detorio MA, Liang B, Kleinhenz DJ, Walp ER, Dikalov S, Jones DP, Schinazi RF, Sutliff RL (2009) Long-term exposure to AZT, but not d4T, increases endothelial cell oxidative stress and mitochondrial dysfunction. Cardiovasc Toxicol 9:1–12

Lewis W, Kohler JJ, Hosseini SH, Haase CP, Copeland WC, Bienstock RJ, Ludaway T, McNaught J, Russ R, Stuart T, Santoianni R (2006) Antiretroviral nucleosides, deoxynucleotide carrier and mitochondrial DNA: evidence supporting the DNA pol gamma hypothesis. AIDS 20:675–684

Maagaard A, Kvale D (2009) Mitochondrial toxicity in HIV-infected patients both off and on antiretroviral treatment: a continuum or distinct underlying mechanisms? J Antimicrob Chemother 64:901–909

Maagaard A, Holberg-Petersen M, Kollberg G, Oldfors A, Sandvik L, Bruun JN (2006) Mitochondrial (mt)DNA changes in tissue may not be reflected by depletion of mtDNA in peripheral blood mononuclear cells in HIV-infected patients. Antivir Ther 11:601–608

Mahajan SD, Roy I, Xu G, Yong KT, Ding H, Aalinkeel R, Reynolds J, Sykes D, Nair BB, Lin EY, Prasad PN, Schwartz SA (2010) Enhancing the delivery of anti retroviral drug "Saquinavir" across the blood brain barrier using nanoparticles. Curr HIV Res 8:396–404

Manda VK, Mittapalli RK, Bohn KA, Adkins CE, Lockman PR (2010) Nicotine and cotinine increases the brain penetration of saquinavir in rat. J Neurochem 115:1495–1507

Masliah E, Ge N, Morey M, DeTeresa R, Terry RD, Wiley CA (1992) Cortical dendritic pathology in human immunodeficiency virus encephalitis. Lab Invest 66:285–291

Moyle G (2005) Mechanisms of HIV and nucleoside reverse transcriptase inhibitor injury to mitochondria. Antivir Ther 10(Suppl 2): M47–M52

Opii WO, Sultana R, Abdul HM, Ansari MA, Nath A, Butterfield DA (2007) Oxidative stress and toxicity induced by the nucleoside reverse transcriptase inhibitor (NRTI)—2′,3′-dideoxycytidine (ddC): relevance to HIV-dementia. Exp Neurol 204:29–38

Prabhakar K, Afzal SM, Kumar PU, Rajanna A, Kishan V (2011) Brain delivery of transferrin coupled indinavir submicron lipid emulsions—pharmacokinetics and tissue distribution. Colloids Surf B Biointerfaces 86:305–313

Robertson KR, Smurzynski M, Parsons TD, Wu K, Bosch RJ, Wu J, McArthur JC, Collier AC, Evans SR, Ellis RJ (2007) The prevalence and incidence of neurocognitive impairment in the HAART era. AIDS 21:1915–1921

Robertson KR, Su Z, Margolis DM, Krambrink A, Havlir DV, Evans S, Skiest DJ (2010) Neurocognitive effects of treatment interruption in stable HIV-positive patients in an observational cohort. Neurology 74:1260–1266

Sacktor N, Lyles RH, Skolasky R, Kleeberger C, Selnes OA, Miller EN, Becker JT, Cohen B, McArthur JC (2001) HIV-associated neurologic disease incidence changes: Multicenter AIDS Cohort Study, 1990–1998. Neurology 56:257–260

Sacktor N, McDermott MP, Marder K, Schifitto G, Selnes OA, McArthur JC, Stern Y, Albert S, Palumbo D, Kieburtz K, De Marcaida JA, Cohen B, Epstein L (2002) HIV-associated cognitive impairment before and after the advent of combination therapy. J Neurovirol 8:136–142

Saitoh A, Fenton T, Alvero C, Fletcher CV, Spector SA (2007) Impact of nucleoside reverse transcriptase inhibitors on mitochondria in human immunodeficiency virus type 1-infected children receiving highly active antiretroviral therapy. Antimicrob Agents Chemother 51:4236–4242

Saitoh A, Haas RH, Naviaux RK, Salva NG, Wong JK, Spector SA (2008) Impact of nucleoside reverse transcriptase inhibitors on mitochondrial DNA and RNA in human skeletal muscle cells. Antimicrob Agents Chemother 52:2825–2830

Saiyed ZM, Gandhi NH, Nair MP (2010) Magnetic nanoformulation of azidothymidine 5'-triphosphate for targeted delivery across the blood–brain barrier. Int J Nanomedicine 5:157–166

Saksena NK, Smit TK (2005) HAART & the molecular biology of AIDS dementia complex. Indian J Med Res 121:256–269

Schnell G, Spudich S, Harrington P, Price RW, Swanstrom R (2009) Compartmentalized human immunodeficiency virus type 1 originates from long-lived cells in some subjects with HIV-1-associated dementia. PLoS Pathog 5:e1000395

Schnell G, Price RW, Swanstrom R, Spudich S (2010) Compartmentalization and clonal amplification of HIV-1 variants in the cerebrospinal fluid during primary infection. J Virol 84:2395–2407

Smit TK, Brew BJ, Tourtellotte W, Morgello S, Gelman BB, Saksena NK (2004) Independent evolution of human immunodeficiency virus (HIV) drug resistance mutations in diverse areas of the brain in HIV-infected patients, with and without dementia, on antiretroviral treatment. J Virol 78:10133–10148

Takeuchi H, Mizuno T, Zhang G, Wang J, Kawanokuchi J, Kuno R, Suzumura A (2005) Neuritic beading induced by activated microglia is an early feature of neuronal dysfunction toward neuronal death by inhibition of mitochondrial respiration and axonal transport. J Biol Chem 280:10444–10454

Venhoff N, Setzer B, Melkaoui K, Walker UA (2007) Mitochondrial toxicity of tenofovir, emtricitabine and abacavir alone and in combination with additional nucleoside reverse transcriptase inhibitors. Antivir Ther 12:1075–1085

Villa G, Solida A, Moro E, Tavolozza M, Antinori A, De Luca A, Murri R, Tamburrini E (1996) Cognitive impairment in asymptomatic stages of HIV infection. A longitudinal study. Eur Neurol 36:125–133

Wang GJ, Nutter LM, Thayer SA (1997) Insensitivity of cultured rat cortical neurons to mitochondrial DNA synthesis inhibitors: evidence for a slow turnover of mitochondrial DNA. Biochem Pharmacol 54:181–187